Pergamon

Tetrahedron 56 (2000) 3691–3695

TETRAHEDRON

Revised Structure of Antidesmone, an Unusual Alkaloid from Tropical *Antidesma* Plants (Euphorbiaceae)

Gerhard Bringmann,[a,*] Jan Schlauer,[a] Heiko Rischer,[a] Michael Wohlfarth,[a] Jörg Mühlbacher,[a] Alexander Buske,[b] Andrea Porzel,[b] Jürgen Schmidt[b] and Günter Adam[b]

[a]*Institut für Organische Chemie, Universität Würzburg, Am Hubland, D-97074 Würzburg, Germany*
[b]*Institut für Pflanzenbiochemie, Abteilung Naturstoffchemie, Postfach 110432, D-06018 Halle/Saale, Germany*

Received 9 March 2000; accepted 10 April 2000

Abstract—The structure of antidesmone, an alkaloid from *Antidesma membranaceum* Müll. Arg. and *A. venosum* E. Mey. (Euphorbiaceae), was revised to be (*S*)-4,8-dioxo-3-methoxy-2-methyl-5-*n*-octyl-1,4,5,6,7,8-hexahydroquinoline [(*S*)-**2**], not the isoquinoline derivative **1**, as assumed previously. The revision was initiated by biosynthetic feeding experiments of one of our groups.

Introduction

Recently, a novel bicyclic alkaloid, named antidesmone, was isolated from the East African Euphorbiaceae species *Antidesma membranaceum* Müll. Arg.[1] The attribution of its constitution was based on the following argumentation: The presence of an *n*-octyl side chain was established by HREIMS. From ^{1}H and ^{13}C 1- and 2D NMR experiments (HSQC, HMBC, COSY, NOESY), a substituted cyclohexenone ring with a pseudo-axial side chain opposite to the carbonyl function and an N–C(CH_3)=C(OCH_3) fragment were deduced. From the molecular formula $C_{19}H_{29}NO_3$, as obtained from HREIMS, this fragment was recognized to be part of an unsaturated second ring. This ring, which was found to carry yet another oxygen function, was interpreted to be annulated to the cyclohexenone ring in a way to give the overall structure **1**, i.e. that of 1-hydroxy-4-methoxy-3-methyl-5-*n*-octyl-8-oxo-5,6,7,8-tetrahydroisoquinoline (Fig. 1). The determination of this connectivity within the nitrogen-containing heterocycle and its constitutional relation to the isocycle was critical because no HMBC or NOE correlations between the two parts of the molecule were observed, which was further complicated by the fact that only low quantities of antidesmone were available from the plant material. The proximity of the two oxygen functions at C-1 and C-8 of the postulated structure **1** was believed to be plausible by the presumed formation of a cyclic boronic diester after reduction of the carbonyl function at C-8, which was deduced from GC-MS experiments.[2] Based on this structural attribution **1** (Fig. 1) by the Halle group, quantum chemical CD-calculations by the Würzburg group gave a CD curve suggesting *S*-configuration for that constitution. In the course of more recent investigations on the biogenesis of antidesmone, the Würzburg group demonstrated the constitution **1** to be incorrect, and showed that antidesmone is represented by structure **2** (Fig. 1).[3] Accordingly, antidesmone is a quinoline, not an isoquinoline alkaloid. In this paper, we describe the revised structure **2**

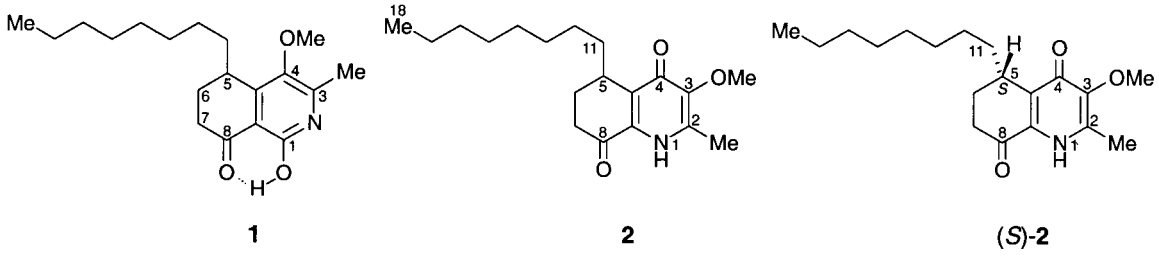

1 **2** (*S*)-**2**

Figure 1. Antidesmone: erroneous structure **1**, revised constitution **2**, and revised absolute stereostructure (*S*)-**2**.

Keywords: antidesmone; quinoline alkaloids; *Antidesma*; Euphorbiaceae; structural elcuidation.
* Corresponding author. Tel.: +49-931-888-5323; fax: +49-931-888-4755; e-mail: bringman@chemie.uni-wuerzburg.de

0040–4020/00/$ - see front matter
PII: S0040-4020(00)00289-1

for antidesmone, here based on the reexamination of a newly isolated sample of the alkaloid, including an investigation of its *O*- and *N*-methylated derivatives. Based on this revised constitution, quantum chemical CD calculations clearly indicate antidesmone to have *S*-configuration, i.e. to be represented by structure (*S*)-**2**.

Results and Discussion

Antidesmone was isolated by a procedure similar to the one described earlier.[1] In those previous investigations, no critical HMBC interactions had been found between the isocyclic ring and the heteroaromatic one (except for the bridgehead C-atoms). In a renewed, now long-term HMBC experiment with a microprobe and using a larger amount (9 mg) of newly isolated antidesmone, a weak, but significant correlation between 5-H (at δ 3.27 ppm) and the carbon atom at δ 172.8 ppm (which is thus C-4, not C-1) could be observed, thus disproving structure **1** of antidesmone and supporting the new constitution **2** (Fig. 2; for further correlations, see Table 1), in agreement with the results of biosynthetic feeding experiments in Würzburg.[3]

To support these findings independently of the aforementioned experiments, the synthesis and NMR investigation of the *O*- and *N*-methyl analogs **3** and **4** of antidesmone (Fig. 3) seemed to be rewarding. These derivatives were obtained in a 3:1 ratio by reaction of antidesmone (3 mg) with diazomethane in diethyl ether. Both **3** and **4** showed molecular ions at *m/z* 333 in the EI mass spectra and $[M+H]^+$ ions at *m/z* 334 in the ESI mass spectra. Their identical molecular formulae of $C_{20}H_{31}NO_3$ were determined by HREIMS. The

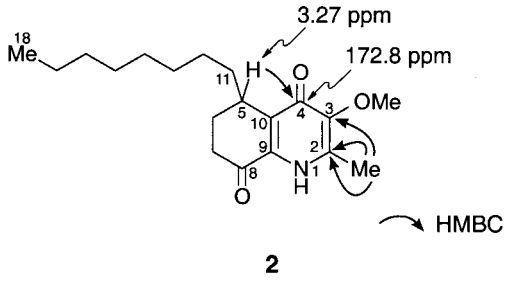

Figure 2. Selected ^1H and ^{13}C NMR shifts as well as HMBC correlations for antidesmone.

Table 1. Observed HMBC correlations of compounds **2**, **3**, and **4** (n.d.=not detected)

Position of H-atoms	Correlations to C-atoms		
	2	**3**	**4**
5-H	4, 6, 7, 9, 10, 11, 12	4, 6, 7, 9, 10	n.d.
6-H_{ax}	5, 7, 8, 10, 11	5, 7, 8, 10, 11	n.d.
6-H_{eq}	5, 7, 8, 10, 11	5, 7, 8, 10, 11	n.d.
7-H_{ax}	5, 6, 8	5, 6, 8	n.d.
7-H_{eq}	5, 6, 8, 9	5, 6, 8, 9	n.d.
2-Me	2, 3	2, 3	2, 3
3-OMe	3	3	3
11-H	5, 6, 10, 12	5, 6, 10, 12, 13	n.d.
18-H	16, 17	16, 17	16, 17
4-OMe	–	4	–
NMe	–	–	2, 9

^1H NMR spectrum of **3** (Fig. 3) showed four proton signals corresponding to methyl groups at δ 4.01 ppm (s), 3.85 ppm (s), 2.56 ppm (s) and 0.89 ppm (t, J=7.2 Hz, not shown in Fig. 3). As indicated by the shifts of the corresponding ^{13}C signals (δ 60.3 and 60.1 ppm) obtained from the HSQC spectrum, the two signals at δ 4.01 ppm and δ 3.85 ppm belong to methoxy groups. Besides the four mentioned methyl signals, the DEPT-135 spectrum showed one methine signal (C-5, δ 31.5 ppm) and 9 methylene signals, while the $^{13}C\{^1H\}$ spectrum indicated the presence of six quarternary carbons. The connectivities of the protons of the cyclohexenone ring were determined by analysis of the $^1H,^1H$ coupling constants. The vicinal coupling constant between the axial proton at C-6 (δ 2.12 ppm) and 5-H (δ 3.21 ppm) with a coupling constant of 4.8 Hz, as obtained from selective homo-decoupling experiments, strongly indicated a pseudo-equatorial orientation of 5-H. This is supported by the observed W-type long-range coupling between 7-H_{eq} and 5-H (^4J=0.7 Hz). The assignment of the proton and carbon signals of the cyclohexenone ring and the *n*-octyl sidechain were established on the basis of ^1H, ^{13}C long-range correlations (Table 1). Like in the case of antidesmone itself, the HMBC spectrum of **3** showed only two correlations of the protons of 2-Me (δ 2.56 ppm) with the carbon signals at δ 154.1 ppm (C-2) and δ 149.1 ppm (C-3). The latter also shared an HMBC correlation with the methoxy protons of 3-OMe. Furthermore, in the NOE difference spectrum of **3**, irradiation of 2-Me resulted in an enhancement of the methoxy signal at δ 3.85 ppm, which was therefore clearly proven to be 3-OMe. The NOE observed between 3-OMe and the second, newly introduced *O*-methyl group at δ 4.01 ppm (4-OMe), however, disagreed significantly with the structure **1** of antidesmone previously assumed.[1] Moreover, an HMBC correlation between the carbon signal at δ 155.8 (C-4) and both of the proton signals at δ 4.01 (4-OMe) and δ 3.21 (5-H) as well as the NOE observed between these two latter proton

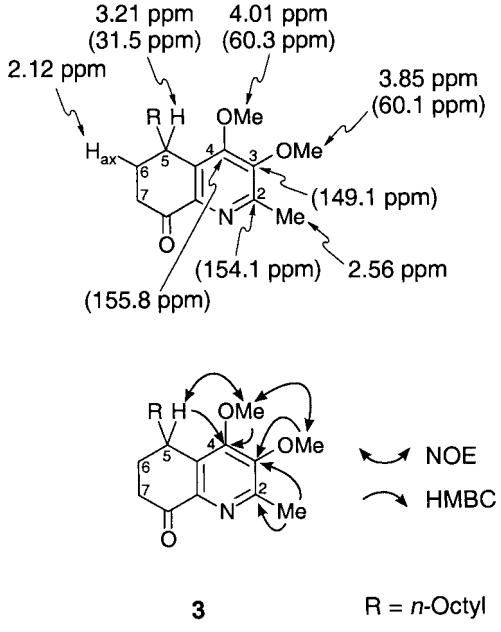

Figure 3. Selected ^1H and ^{13}C (in parentheses) NMR shifts as well as HMBC and NOE correlations in **3**.

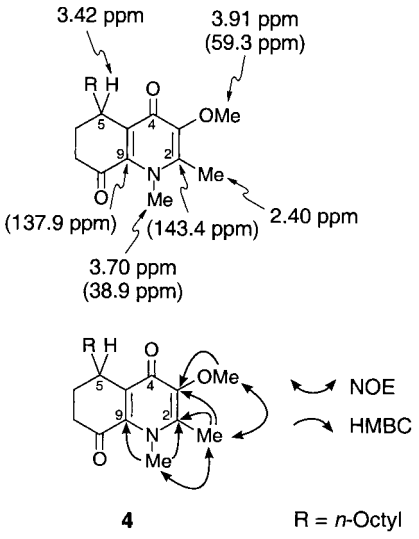

Figure 4. Selected ^{1}H and ^{13}C (in parentheses) NMR shifts as well as HMBC and NOE correlations in **4**.

signals indicated their close spatial proximity (Fig. 3). All these spectral data clearly showed the product to be *O*-methylantidesmone and to possess the constitution **3**, which thus unambiguously established **2** as the correct constitution of the natural product, antidesmone.

This constitution of antidesmone was also confirmed by the spectroscopic data of its *N*-methyl derivative **4** (Fig. 4). The ^{1}H NMR spectrum of **4** displayed four methyl signals at δ 3.91 ppm (s), 3.70 ppm (s), 2.40 ppm (s) and 0.87 ppm (t, J=7.0 Hz, not shown in Fig. 4), with a close resemblance to the spectrum of **3**. However, the HSQC correlations of the two downfield methyl signals (δ 3.91 ppm and δ 3.70 ppm) with the carbon signals at 59.3 and 38.9 ppm, respectively, clearly excluded the presence of two *O*-methyl groups and rather suggested the existence of an *O*-methyl and an *N*-methyl group. As indicated by the HMBC correlation signals of the methyl protons at δ 3.70 ppm with both carbon signals at δ 143.4 ppm (C-2) and δ 137.9 ppm (C-9), and from the ^{13}C NMR shift of that methyl group (38.9 ppm), it is attached to the nitrogen in the unsaturated ring. This was further confirmed by the NOE effects observed between 2-Me (δ 2.40 ppm) and both, the methoxy group at C-3 (δ 3.91 ppm) and that *N*-methyl group (δ 3.70 ppm). From the ^{13}C chemical shifts of the two sp^2 carbon atoms bound to the nitrogen atom (δ 143.4 and 137.9 ppm), it became evident that neither could be a carbonyl carbon, thus excluding a 2-pyridone structure for the nitrogen containing ring of **4**. For further HMBC-correlations, see Table 1.

With the constitution of antidesmone now unambiguously established as **2**, it seemed rewarding to likewise assign its absolute configuration, here by molecular dynamics (MD) based quantum chemical CD calculations according to procedures elaborated earlier.[4–6] Because of the possible existence of a hydroxypyridine-pyridone tautomeric equilibrium mixture for **2**, we decided to perform the molecular dynamics simulation and the CD calculation not on **2** itself, but on a methylated derivative, in which one of the two tautomeric forms is fixed. Due to its lower flexibility compared to that of the 4-*O*-methyl derivative **3**, the *N*-methylated derivative **4** was chosen for this theoretical investigation.

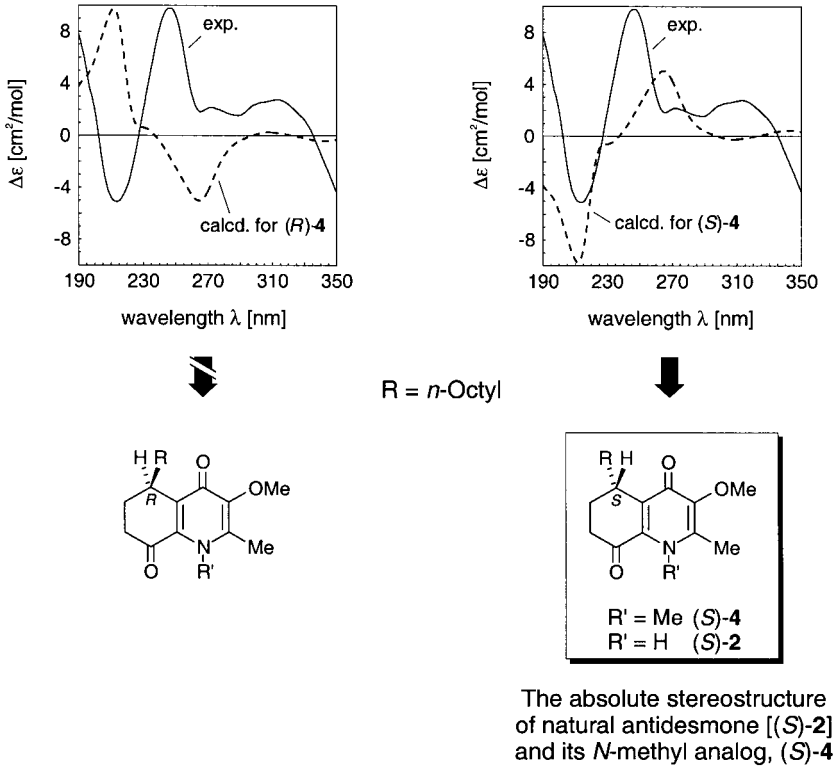

Figure 5. Stereochemical assignment of antidesmone as (*S*)-**2**, by MD-based calculated CD spectra predicted for the two possible enantiomers of **4** and comparison with the experimental one.

Arbitrarily starting with the *R*-enantiomer of **2**, molecular dynamics (MD) simulations using the TRIPOS force field[7] were performed for 500 ps, recording the geometry every 0.5 ps for further calculations. For all of the 1000 structures thus collected, single CD spectra were calculated. The computed spectra were averaged arithmetically over the trajectory to give the theoretical overall spectrum. In order to take into account a systematic shift of the calculated CD spectrum, a 'UV correction'[4] was carried out. As shown in Fig. 5, the theoretical spectrum thus predicted for (*R*)-**2** is nearly opposite to the experimental one, while the CD spectrum calculated for the *S*-enantiomer shows a good agreement and establishes the *N*-methylated product **4**—and thus also **2**—to be *S*-configured (Fig. 5). Thus, the natural product antidesmone is represented by the full absolute stereostructure (*S*)-**2**.

Antidesmone [(*S*)-**2**] is structurally closely related to hyeronimone,[8] a similar quinoline alkaloid from the roots of *Hyeronima alchorneoides* (likewise Euphorbiaceae), which is a dihydro form of **2**. From *H. oblonga*, by contrast, two related compounds, hyeronines A and B, were reported to be isoquinoline derivatives.[9] Of these, hyeronine A, although considered as an alkaloid related to structure **1**, yet with an *n*-octanoyl side chain at C-6, might likewise be a quinoline, not an isoquinoline alkaloid.

Experimental

^{1}H, 1D NOE difference spectra and 2D spectra were recorded on a Varian Unity 500 spectrometer at 499.8 MHz in $CDCl_3$ with TMS as the internal reference. The coupling constants, *J*, are given in Hertz. $^{13}C\{^1H\}$ and DEPT-135 spectra were recorded on a Varian Unity 500 spectrometer at 125.7 MHz in $CDCl_3$, with the solvent signal (δ 77.0 ppm) as the internal reference. High resolution mass spectra were acquired on an MAT 90 mass spectrometer at 70 eV (EI). GC-EIMS analyses were carried out on an MD-800 system (Fisons Instruments) at 70 eV with a source temperature of 200°C. The column used was a DB-5MS (J&W, 15 m×0.32 mm, 0.25 μm film thickness) at an injection temperature of 250°C (splitless injection), an interface temperature of 300°C with a carrier gas (He) flow rate of 1 ml/min. The temperature program was as follows: 60°C for 1 min, then raised to 110°C at a rate of 25°C min^{-1} and then to 290°C at a rate of 10°C min^{-1}. HPLC-MS analyses were carried out on a Finnigan TSQ 7000 in the positive ESI mode (4.5 kV spray voltage), equipped with LC-Tech Ultra Plus pumps and a Linear UVIS 200 detector. Chromatographic separation was carried out on a Sepserve Ultrasep ES RP-18 (1×100 mm, 5 μm particle size) column at a flow rate of 70 μl min^{-1} (gradient: 50% acetonitrile in 15 min to 90% acetonitrile, 0.2% HOAc). The CD spectra were recorded in ethanolic solution on a J-715 spectropolarimeter (JASCO, Gross-Umstadt, Germany) at room temperature within the range of 190 to 400 nm. IR spectra were acquired on a 1600 Series FTIR spectrometer (Perkin–Elmer, Überlingen, Germany).

Plant material

Leaf material of *A. venosum* was collected in August 1999 in Dar es Salaam, Tanzania, by L. B. Mwasumbi and B. A. O. Mponda. A voucher specimen is deposited in The Herbarium, University of Dar es Salaam (No. LBM 113000).

Isolation of antidesmone [(*S*)-2]

Dry leaves (939 g) were extracted with 90% MeOH (3×10 l for 24 h at room temperature). This extract was reduced in vacuo to one third of its original volume, defatted with *n*-hexane (3×1 l), reduced to the aqueous phase (1 l), diluted with 1 l MeOH, and extracted with $CHCl_3$/*n*-hexane (80:20, 5 l). The organic layer was taken to dryness (6.5 g) and fractionated using CC (250 g silica gel, *n*-hexane with increasing amounts of ethyl acetate). The fraction containing (*S*)-**2** (*n*-hexane:ethyl acetate 50:50 to 20:80, 0.32 g) was further purified by preparative HPLC (Merck-Hitachi D-6000 System, Hibar 25×250 mm, LiChrosorb RP-18, 7 mm, MeOH:H_2O gradient from 66% MeOH to 100% MeOH in 20 min, flow: 10 ml min^{-1}), yielding 37.4 mg of (*S*)-**2**, identical in all respects with antidesmone previously isolated from *A. membranaceum*.[1]

Antidesmone [(*S*)-2]

Pale yellow oil; UV (MeOH): λ_{max} 247 (log ϵ 4.21), 275 (log ϵ 3.44), 327 (log ϵ 3.52); CD: $\Delta\epsilon_{212}$ −4.38, $\Delta\epsilon_{246}$ 5.63, $\Delta\epsilon_{279}$ 1.87, $\Delta\epsilon_{315}$ 2.36, $\Delta\epsilon_{354}$ −319; IR (NaCl): $\tilde{\nu}$ 3180 (OH), 2900, 2815 (C-H), 1775 (C=O), 1595, 1535, 1500, 1440, 1385, 1340, 1260, 1190, 1165, 1025; ^{1}H NMR (500 MHz, $CDCl_3$): δ=0.87 (t, *J*=7.0 Hz, 3H, 18-H), 1.2–1.4 (6H, 13-H, 14-H, 15-H, overlapping), 1.25 (2H, 16-H, overlapping), 1.26 (2H, 17-H, overlapping), 1.41 (1H, 11-H, overlapping), 1.46 (2H, 12-H, overlapping), 1.77 (m, 1H, 11-H), 2.08 (dddd, *J*=14.7, 14.0, 4.7, 4.4 Hz, 1H, 6-H_{ax}), 2.20 (dddd, *J*=14.0, 5.3, 2.4, 2.4 Hz, 1H, 6-H_{eq}), 2.37 (s, 3H, 2-Me), 2.58 (ddd, *J*=18.2, 4.4, 2.4 Hz, 1H, 7-H_{eq}), 2.75 (ddd, *J*=18.2, 14.7, 5.3 Hz, 1H, 7-H_{ax}), 3.27 (br s, 1H, 5-H), 3.94 (s, 3H, 3-OMe); ^{13}C NMR (125 MHz, $CDCl_3$): δ=14.0 (C-18), 14.5 (2-Me), 22.6 (C-17), 24.3 (C-6), 28.4 (C-12), 29.2, 29.5, 29.6 (C-13, C-14, C-15), 30.3 (C-5), 30.5 (C-11), 31.8 (C-16), 32.2 (C-7), 59.4 (3-OMe), 132.2 (C-9), 138.9 (C-2), 139.0 (C-10), 147.5 (C-3), 172.8 (C-4), 194.6 (C-8); EIMS *m/z* (rel. int.) 318 ($[M-H]^+$), 5), 292 (12), 234 ($[M-C_6H_{13}]^+$, 26), 206 ($[M-C_8H_{17}]^+$, 26), 189 (10), 178 (9), 164 (6).

Methylation of (*S*)-2

3 mg (9.4 mmol) **2** were reacted with a solution of diazomethane in ether (3 ml) for 4 h at room temperature. After evaporation of the solvent the resulting mixture was purified by preparative HPLC to yield **3** (1.9 mg, 61%) and **4** (0.7 mg, 22%) as amorphous yellowish solids.

4-*O*-Methylantidesmone (3)

UV (MeOH): λ_{max} 214 (log ϵ 4.23), 262 (log ϵ 3.63), 290 (log ϵ3.62); CD: $\Delta\epsilon_{199}$ 4.60, $\Delta\epsilon_{223}$ −1.67, $\Delta\epsilon_{255}$ 0.82, $\Delta\epsilon_{283}$ −0.09, $\Delta\epsilon_{290}$ 0.01, $\Delta\epsilon_{330}$ −0.99; IR (NaCl): $\tilde{\nu}$ 2925, 2854 (C-H), 1701 (C=O), 1574, 1458, 1404, 1348, 1226, 1092, 1073; ^{1}H NMR (500 MHz, $CDCl_3$): δ=0.89 (t, *J*=7.0 Hz, 3H, H-18), 1.25–1.40 (6H, 13-H, 14-H, 15-H, overlapping), 1.27 (2H, 16-H, overlapping), 1.28 (m, 2H, 17-H,

overlapping), 1.36 (1H, 12-H, overlapping), 1.49 (1H, 12-H, overlapping), 1.53 (1H, 11-H, overlapping), 1.61 (1H, 11-H, overlapping), 2.12 (dddd, J=14.0, 14.0, 5.0, 4.5 Hz, 1H, 6-H_{ax}), 2.17 (dddd, J=14.0, 6.0, 3.0, 2.5 Hz, 1H, 6-H_{eq}), 2.55 (s, 3H, 2-Me), 2.67 (dddd, J=18.0, 4.5, 2.5, 0.7 Hz, 1H, 7-H_{eq}), 2.80 (ddd, J=18.0, 14.0, 6.0 Hz, 1H, 7-H_{ax}), 3.22 (m, 1H, 5-H), 3.85 (s, 3H, 3-OMe), 4.01 (s, 3H, 4-OMe); ^{13}C NMR (125 MHz, $CDCl_3$): δ=14.1 (C-18), 19.5 (2-Me), 22.7 (C-17), 24.4 (C-6), 28.1 (C-12), 29.3, 29.4, 29.5 (C-13, C-14, C-15), 31.5 (C-5), 31.9 (C-16), 32.7 (C-11), 33.8 (C-7), 60.1 (3-OMe), 60.3 (4-OMe), 138.9 (C-10), 143.0 (C-9), 149.1 (C-3), 154.1 (C-2), 155.8 (C-4), 196.3 (C-8); HPLC-ESIMS: t_R=20.30 min, m/z (rel. int.) 334 ($[M+H]^+$, 100); GC-EIMS: t_R=16.69 min, m/z (rel. int.) 333 (M^+, 2), 332 ($[M-H]^+$, 3), 318 (6), 305 (15), 302 ($[M-H-CH_2O]^+$, 12), 290 (4), 277 (12), 274 (8), 262 (5), 248 (14), 234 (43), 221 (33), 220 ($[M-C_8H_{17}]^+$, 100), 207 (13), 206 (47), 192 (61), 177 (29), 176 (28), 162 (9), 159 (15), 148 (16); Exact mass calcd for $C_{20}H_{31}NO_3^+$ 333.2304. Found: 333.2297.

N-Methylantidesmone (4)

UV (MeOH): λ_{max} 199 (log ϵ 3.77), 248 (log ϵ 3.84), 277 (log ϵ 3.24), 330 (log ϵ 3.36); CD: $\Delta\epsilon_{197}$ 1.06, $\Delta\epsilon_{210}$ −1.20, $\Delta\epsilon_{247}$ 2.01, $\Delta\epsilon_{310}$ 0.53, $\Delta\epsilon_{357}$ −0.99; IR (NaCl): $\tilde{\nu}$ 2924, 2852 (C–H), 1734 (C=O), 1691, 1594, 1560, 1462, 1418, 1385, 1352, 1290, 1266, 1165, 1132, 1099; ^{1}H NMR (500 MHz, $CDCl_3$): δ=0.87 (t, 7.0 Hz, 3H, 18-H), 1.24 (2H, 16-H, overlapping), 1.25–1.40 (6H, 13-H, 14-H, 15-H, overlapping), 1.33 (1H, 11-H, overlapping), 1.40 (1H, 12-H, overlapping), 1.45 (1H, 12-H, overlapping), 1.27 (2H, 17-H, overlapping), 1.64 (1H, 11-H, overlapping), 2.03 (dddd, J=14.0, 14.0, 5.5, 4.5 Hz, 1H, 6-H_{ax}), 2.11 (dddd, J=14.0, 6.0, 2.5, 2.0 Hz, 1H, 6-H_{eq}), 2.40 (s, 3H, 2-Me), 2.59 (ddd, J=18.0, 6.0, 2.0 Hz, 1H, 7-H_{eq}), 2.81 (ddd, J=18.0, 14.0, 6.0 Hz, 1H, 7-H_{ax}), 3.42 (m, 1H, 5-H), 3.70 (s, 3H, NMe), 3.91 (s, 3H, 3-OMe), ^{13}C NMR (125 MHz, $CDCl_3$): δ=13.4 (2-Me), 14.1 (C-18), 22.7 (C-17), 23.6 (C-6), 28.4 (C-12), 29.3, 29.6, 29.7 (C-13, C-14, C-15), 31.1 (C-5), 31.3 (C-11), 31.9 (C-16), 35.6 (C-7), 38.9 (NMe), 59.3 (3-OMe), 137.9 (C-9), 142.3 (C-10), 143.4 (C-2), 147.3 (C-3), 170.8 (C-4), 196.2 (C-8); HPLC-ESIMS: t_R=11.30 min, m/z (rel. int.): 334 ($[M+H]^+$, 100); GC-EIMS: t_R=17.65 min, m/z (rel. int.): 333 (M^+, 7), 332 ($[M-H]^+$, 7), 318 (7), 305 (38), 304 (11), 290 (9), 277 (17), 276 (9), 262 (9), 248 (53), 234 (54), 222 (40), 221 ($[M-C_8H_{16}]^+$, 100), 207 (43), 206 (48), 203 (51), 193 (44), 192 (52), 178 (47), 175 (34), 162 (15), 160 (13), 148 (14); Exact mass calcd for $C_{20}H_{31}NO_3^+$ 333.2304. Found: 333.2300.

Computational

Molecular dynamics

The MD simulation was performed on Silicon Graphics Octane R10000 workstations using the TRIPOS[7] force field as implemented in the molecular modelling package SYBYL.[7] The molecule was weakly coupled to a virtual thermal bath at T=400 K,[10] with a temperature relaxation time τ=0.12 ps.

CD calculations

The wavefunctions for the calculation of the rotational strengths for the electronic transitions from the ground state to excited states were obtained by a CNDO/S-CI[11,12] calculation, in which the CI expansion takes into account the ground state and all n and π orbitals. These calculations were carried out on Linux *i*PII and *i*PIII workstations using the BDZDO/MCDSPD[11] program package. For a better comparison of the theoretical CD spectrum with the experimental one, a Gaussian band shape function was generated over the calculated rotational strength values.

Acknowledgements

This work was supported by the Deutsche Forschungsgemeinschaft (SFB 251 'Ökologie, Physiologie und Biochemie pflanzlicher und tierischer Leistung unter Stress'), the Max-Buchner-Forschungsstiftung (grants for M. W. and H. R.), and by the Fonds der Chemischen Industrie. The authors are indebted to Mr L. B. Mwasumbi (Dar es Salaam, Tanzania) for providing the plant material and to Prof C. L. Zani for a genuine sample of hyeronine A. Furthermore, we wish to thank Prof J. Fleischhauer (University of Aachen), Prof J. Michl, and Dr. J. W. Downing (University of Colorado) for providing the program package BDZDO/MCDSPD and to Dr K.-P. Gulden for porting it to LinuX.

References

1. Buske, A.; Busemann, S.; Mühlbacher, J.; Schmidt, J.; Porzel, A.; Bringmann, G.; Adam, G. *Tetrahedron* **1999**, *55*, 1079–1086.
2. In the light of the results presented here, the boronic ester product was probably rather an oxazaborolidine derivative formed from the OH group at C-8 and the NH function.
3. Bringmann, G.; Rischer, H.; Wohlfarth, M.; Schlauer, J. in preparation.
4. Bringmann, G.; Busemann, S. In *Natural Product Analysis*; Schreier, P., Herderich, M., Humpf, H. U., Schwab, W., Eds.; Vieweg: Braunschweig, 1998; pp 195–212.
5. Dreyer, M.; Nugroho, B. W.; Bohnenstengel, F. I.; Wray, V.; Witte, L.; Bringmann, G.; Mühlbacher, J.; Herold, M.; Hung, P. D.; Kiet, L. C.; Proksch, P. *J. Nat. Prod.*, submitted.
6. Bringmann, G.; Günther, C.; Mühlbacher, J.; Gunathilake, M. D. L. P.; Wickramasinghe, A. *Phytochemistry* **2000**, *53*, 409–416.
7. SYBYL: Tripos Associates, 1699 Hanley Road, Suite 303, St. Louis, MO, 63144.
8. Tinto, W. F.; Blyden, G.; Reynolds, W. F.; McLean, S. J. *J. Nat. Prod.* **1991**, *54*, 1309–1313.
9. Alves, T. M. A.; Zani, C. L. *Tetrahedron Lett.* **1999**, *40*, 205–208.
10. Berendsen, H. J. C.; Postma, J. P. M.; van Gunsteren, W. F.; DiNola, A.; Haak, J. R. *J. Chem. Phys.* **1984**, *81*, 3684–3690.
11. Downing, J. W. Program package BDZDO/MCDSPD, Department of Chemistry and Biochemistry, University of Colorado, Boulder, USA; modified by Fleischhauer, J.; Schleker, W.; Kramer, B. ported to LinuX by Gulden, K.-P.
12. Del Bene, J.; Jaffé, H. H. *J. Chem. Phys.* **1968**, *48*, 1807–1813.